Microelectronic Engineering 187–188 (2018) 90–94

Contents lists available at ScienceDirect

Microelectronic Engineering

journal homepage: www.elsevier.com/locate/mee

Research paper

Zero-mode waveguide detection of DNA translocation through FIB-organised arrays of engineered nanopores

T. Auger [a], E. Bourhis [b], J. Donnez [b], A. Durnez [b], J.M. Di Meglio [a], L. Auvray [a], F. Montel [a,c], J. Yates [d], J. Gierak [b,*]

[a] Matière et Systèmes Complexes, Université Paris Diderot & CNRS (UMR 7057), 75205 Paris Cedex 13, France
[b] Centre de Nanosciences et de Nanotechnologies, CNRS, Univ. Paris-Sud, Université Paris-Saclay, C2N – Marcoussis, 91460 Marcoussis, France
[c] Univ Lyon, Ens de Lyon, Univ Claude Bernard, CNRS, Laboratoire de Physique, F-69342 Lyon, France
[d] ITQB NOVA, Av. da República, 2780-157 Oeiras, Portugal

ARTICLE INFO

Article history:
Received 24 October 2017
Received in revised form 4 December 2017
Accepted 5 December 2017
Available online 6 December 2017

Keywords:
Focused ion beam
Zero-mode waveguide
Dielectric films
Biosensor
Silicon nitride
Silicon carbide

ABSTRACT

Zero-mode waveguides (ZMWs) are optical nanostructures fabricated in a thin metallic film capable of confining the excitation volume to the zeptoliter range.
In this work we describe the batch fabrication of a nanopore-based device, based upon high-resolution arrays of nanopores (of various sizes), which is used to directly measure the passage of DNA. In our method, nanopores are fabricated in ultrathin dielectric films with a deposited gold layer. The gold layer on the device induces a zero-mode waveguide illumination at the *cis* end of the nanopores.
The method presented allows for optical detection, in real time, at the level of a single molecule and a single pore. The detection of fluorescently labelled single molecules passing through the pores, measured using an electron multiplying charge coupled device camera, is described. Molecules inside the nanopore were invisible until they reached the volume illuminated by the evanescent field.
This fabrication methodology appears to be very promising for the development and batch fabrication of a new generation of nanopore-based sensor devices.

1. Introduction

Nanopores have been shown to be very efficient devices to detect [1], characterise [2–4] and even sequence macromolecules such as DNA [5]. Most of the studies in the field are based on electrical driving and sensing of translocation events. Recent studies have demonstrated the possibility of using fluorescence and optical detection as an alternative [6–11] to follow the translocation of nucleic acids in solid state nanopores. Electrical and optical events have been shown to correlate precisely in time [12–14]. The major advantage of optical detection is the ability to achieve high parallelisation and specific labelling of the translocated molecules. In this article, we develop a methodology for the high throughput production of optical devices based upon Zero-Mode Waveguides coupled with nanopores.

A zero-mode waveguide (ZMW) is an optical waveguide that directs light energy into a volume (well) that is smaller, in all dimensions, than the wavelength of the illuminating light. ZWMs were originally fabricated in thin metallic films and were designed as electromagnetical attenuators [15]. More recently, pioneering work by Levene and coworkers [16] has shown that ZMWs can be used to isolate and then optically detect individual molecules that diffuse into nanowells. This is due to the fact that each well in the ZMW confines the illuminated volume (at the bottom of the well) to a few zeptoliters. ZMWs have potential as single molecule real time sequencing (SMRT) devices for sequencing DNA (reviewed in [17]). The entry of analyte molecules into the wells of a ZMW is a diffusion-limited process thus occupancy of individual wells is low. Furthermore, the entry and retention of different sized molecules is biased. For example, short DNA molecules are more likely to enter (or less likely to escape) than long molecules. In addition the molecule under analysis then needs to be trapped within the illuminated volume (the evanescent field region) at the bottom of the well in order to be detected or analysed (discussed in [18–20]).

Nanopore-ZMWs (NZMWs) have been introduced relatively recently. A NZMW contains a nanopore in the base of the ZMW well (in the evanescent field region). This allows for reversible electrophoretic focusing of biomolecules when a potential difference is applied across the device. Such NZMWs have been used to trap DNA in individual waveguides to enhance the sensitivity and efficiency of SMRT [18,19].

We have previously used a simple NZMW structure to optically detect translocated particles driven by a pressure gradient [21]. Here this work is expanded upon to demonstrate translocation driven by an applied potential difference. Furthermore, we show that these simple NZMW structures can be fabricated in a high throughput batch process using a gallium focused ion beam (FIB) to fabricate arrays of nanopores within the device. We have used this FIB process to produce NZMWs in

* Corresponding author.
E-mail address: jacques.gierak@lpn.cnrs.fr (J. Gierak).

https://doi.org/10.1016/j.mee.2017.12.005
0167-9317/

gold-coated silicon nitride (SiN) and silicon carbide (SiC). Nanopores of various sizes were produced within these substrates and optical detection of fluorescently labelled DNA molecules was demonstrated. We used nanopores of different sizes to study the relationship between frequency of translocation events and applied voltages and to show how critical voltage evolves with pore diameter.

The methodology demonstrated here is very well suited to the high-throughput batch production of a new generation of nanopore-based sensor devices.

2. Materials and methods

2.1. FIB setup – nanowriter, source and optics

For the nanopore fabrication a high resolution Ga + FIB Nanowriter developed in our laboratory [22] was used. The Nanowriter is based upon a single beam architecture working in conjunction with a laser interferometer controlled stage and patterning engines from Raith GmbH (Germany; http://www.raith.com). In this machine a specific gallium ion emitter device and controls are used. These allow for record on-axis angular intensity (up to 80 μA/str), a long lifetime and very long-term stability that are important parameters for dose control and precise placement of patterned features. The design of the ion optics includes a μm-sized beam-defining aperture at the entrance of the ion optics and two lenses operated to achieve, as routine, sub-10 nm resolution and abrupt current probe distribution profiles. This instrument combines the advantages of a very high resolution FIB system with the accuracy of a high precision laser interferometer stage (2 nm steps) and a high speed (10 MHz) digital pattern generator.

2.2. Membrane containing devices

Two different membrane materials, SiC (Home made in our facility) and Si3N4 (Norcada, Canada; http://www.norcada.com) were tested. In both cases two inch Si-based samples (300 μm thick) were fabricated using a GDSII mask design. Free standing membranes, 50 nm thick, were then covered with a 50 nm thick gold metal film evaporated using a x-low deposition speed to allow grain sizes in the range of a few nm. The sample was first covered with a thin layer of titanium (2 nm) as an adhesion layer and then with gold. Both metals were evaporated using an Plassys MEB550 electron gun machine at low speed (0,2 nm/s for Ti and 0,5 nm/s for Au). After preparation, the samples were loaded into the FIB system. To avoid charge accumulation, a good electrical contact was maintained between the surface gold layer and the sample holder.

2.3. Device fabrication/patterning – navigation, dose – size calibration, processing and characterisation (TEM, SEM)

Precise patterning and automation were required in order to achieve optimum patterning results over the full wafer (~400 membranes). Automated step and repeat writing on each 50 × 50 μm free-standing membranes was controlled by editing a position list (task list) based on calibration test results obtained either directly inside the FIB nanowriter using Scanning Ion Microscopy images (SIM) of the nanopores or externally via SEM, TEM or AFM.

Step 1: Sample containing free-standing membranes is loaded with the etched backside of the wafer facing the incoming ion beam. In this orientation, the edges of each membrane can be detected and used as an alignment feature.

Step 2: A classical 3 point (X, Y, θ) alignment procedure is then used for allowing automated navigation.

Step 3: On a sacrificial set of membranes, a dose calibration array is patterned and then inspected via ion or electron microscopy. For electron microscopy, the sample has to be unloaded from the FIB.

Step 4: Once the optimum ion dose and patterning conditions have been selected and validated, the complete wafer is automatically patterned. Each membrane is drilled with a matrix of 5 × 5 nanopores.

Typical dwell times for the pore size fabrication were found to be in the order of 20–40 ms (Ga + ion, 30 keV, 5–8 pA). The total time for the wafer processing is in the order of 1 h (field alignment and stage displacements/positioning).

Unattended batch processing is desirable to allow for maximum efficiency of system usage with the highest job yield and minimum feature variation.

2.4. Translocation assay. Details of microscope setup, lambda DNA and YOYO labelling

Phage lambda DNA molecules (New England Biolabs, USA) were labelled using a fluorescent intercalating dye (YOYO-1; Thermo Fisher Scientific, USA).

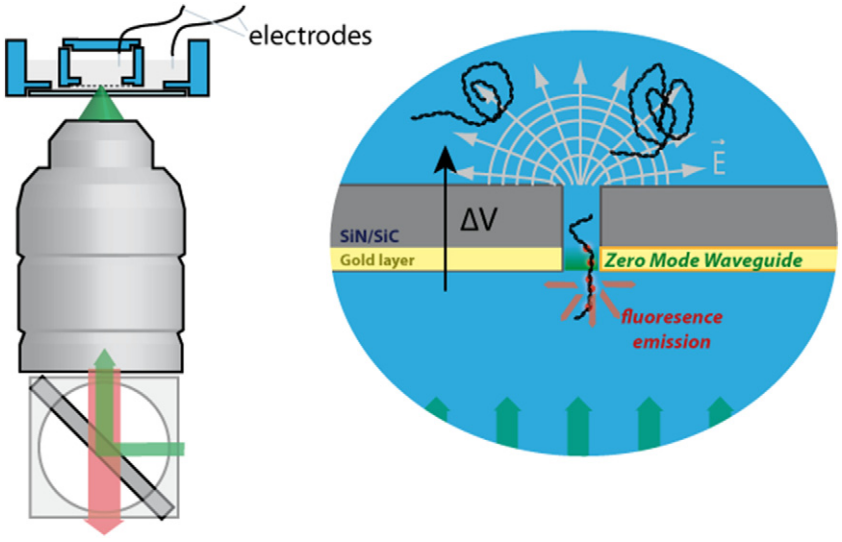

Fig. 1. Experimental setup for the detection of translocation of labelled DNA molecules. Illuminating light is shown in green. Emitted light (fluorescence) is shown in red. In a Zero-Mode Waveguide the fluorescence emission is restrained to the vicinity of the nanopore. DNA molecules are pulled through the nanopore with an electrical field. Translocation events are detected by local fluorescence emission during exit of the molecules.

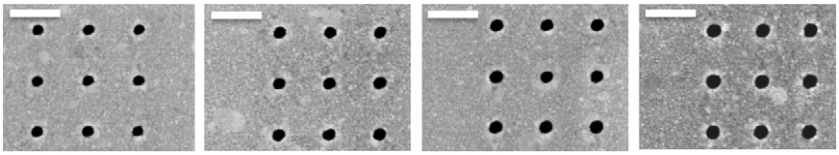

Fig. 2. SEM images of selected nanopores within the NZMW devices. Series of acquired SEM images showing, from left to right: Nanopores with diameters of 100 nm, 130 nm, 140 nm and 170 nm. Nanopores are fabricated in 50 nm thick SiN/SiC membranes covered with a 50 nm thick gold layer. Total thickness of the nanopores is 100 nm. Scale bar is 500 nm.

The optical microscopy setup was composed of a modified inverted fluorescence microscope coupled to a cooled and amplified (single photon sensitivity) camera (Fig. 1). Specifically: a ZEISS Axiovert 200 equipped with a ZEISS water objective (C-Apochromat; magnification of 63×, a numerical aperture of 1.2 and a working distance of 0.28 mm for a 0.17 mm thick glass coverslip), a Micro-Drive microscope-mounted stage (Mad City Labs Inc.) and an iXon 897 EMCCD (Andor Technology Ltd.). Excitation was via a solid-state laser at 488 nm.

A dilute solution of phage λ DNA (1 pM), fluorescently labelled with YOYO-1 in 10 mM KCl, 10 mM Tris buffer pH 7.4 filled the *trans*-chamber of the experimental flow cell. Two Ag/AgCl electrodes, one in each of the *cis* and *trans* chambers, are used to apply a potential difference across the flow cell and generate an ionic current through the nanopores (Fig. 1).

The frequencies of translocation per pore were quantified using a custom MATLAB script and using manual counting of the events and of the number of active pores (see Fig. 3 and also the ¼ speed movie file in the Supplementary information). Frame rate was 30 ms per image. Image backgrounds were reduced by averaging. Each frequency versus voltage curve corresponds to >250 events and were recorded in triplicate that were then averaged to obtain each fitted curve. The error bars were determined from the experimental errors ($\pm\sigma$/sqrt(N) with σ being the standard deviation and $N > 3$ the number of measurements). The robustness of the fitting procedure was assessed by bootstrapping.

3. Results and discussion

3.1. Characterisation of NZMW devices

The individual nanopores patterned within each array were characterised by SEM (representative examples shown in Fig. 2). Diameter and circularity were assessed for each individual nanopore. For each array of nanopores, the stated diameter is the average diameter across all 25 nanopores in the array. Across an array of nanopores, the spread from minimum diameter to maximum diameter was found to be within 10% of the stated diameter. These parameters were judged to be acceptable in terms of both size variation and circularity.

3.2. Translocation of lambda DNA and model

Nanopores, with diameters ranging from 100 nm to 170 nm, were then drilled by FIB in SiC and SiN substrates. Translocation of individual YOYO-1 labelled phage λ DNA molecules through the NZMW devices was observed and quantified (see Fig. 3 and also the movie file in the Supplementary information).

We have characterised the transport of phage λ DNA molecules through nanopores fabricated in gold-coated dielectric films. The frequency of translocation per pore as a function of the voltage (number of events > 250 per curve and number of curves per condition >3, see Materials and methods). Transport through the nanopores was found to be well characterised by the electrical suction model (a generalisation of the de Gennes Brochard model for flow injection) (Fig. 4).

The suction model describes the hydrodynamic injection of macromolecules into nanopores [7]. This model was extended to an electrical driving force. In this case, the energy landscape ΔF for the injection of length X of a DNA tongue (constituted of X/D blobs) into a pore of diameter D and length l by a voltage bias ΔV is given by:

$$\Delta F = k_B T \frac{X}{D} - q_b \frac{\Delta V}{l} \frac{X^2}{D} \quad (1)$$

With q_b the charge per blob of the DNA molecule injected into the pore. The free energy barrier $\Delta F_{\#}$ which corresponds to the local maximum of the landscape is then:

$$\Delta F_{\#} = k_B T \frac{V_c}{\Delta V} \quad (2)$$

With $V_c = \frac{k_B T l}{q_b D}$, the critical voltage bias equivalent to the critical flux in the suction model. The access frequency as described by Kramers

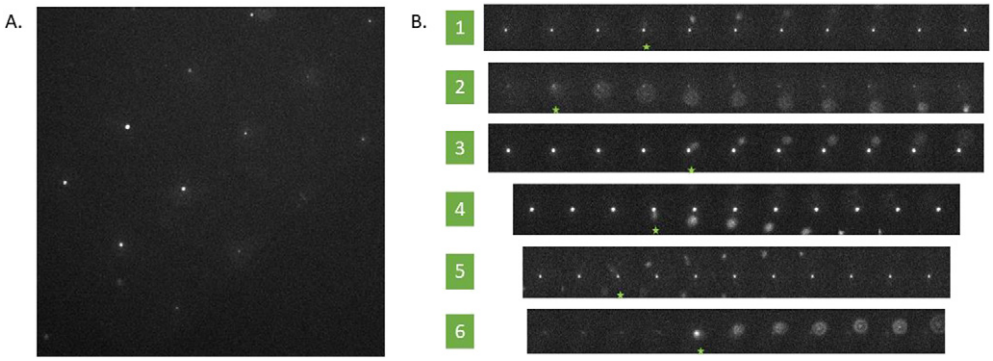

Fig. 3. Observation of transport of phage λ DNA molecules through the NZMW device. A. Nanopore array visualized in fluorescence microscopy. Here the NZMW device consists of 50 nm thick SiC covered with 50 nm thick gold. A 5 × 5 array of 100 nm nanopores was patterned by FIB. The nanopores are visible and appear bright because of the DNA accumulated inside the pore during the experiment. B. Six series of 10 images covering 300 ms. Each image corresponds to a snapshot of an individual DNA translocation event observed in a single pore. A YOYO-1 labelled phage λ DNA molecule is observed as it exits the nanopore (green stars indicate the exit time). Voltage bias is 40 mV. The full video to be found in the Supplementary information. Frame rate is slowed down 4 times in the video.

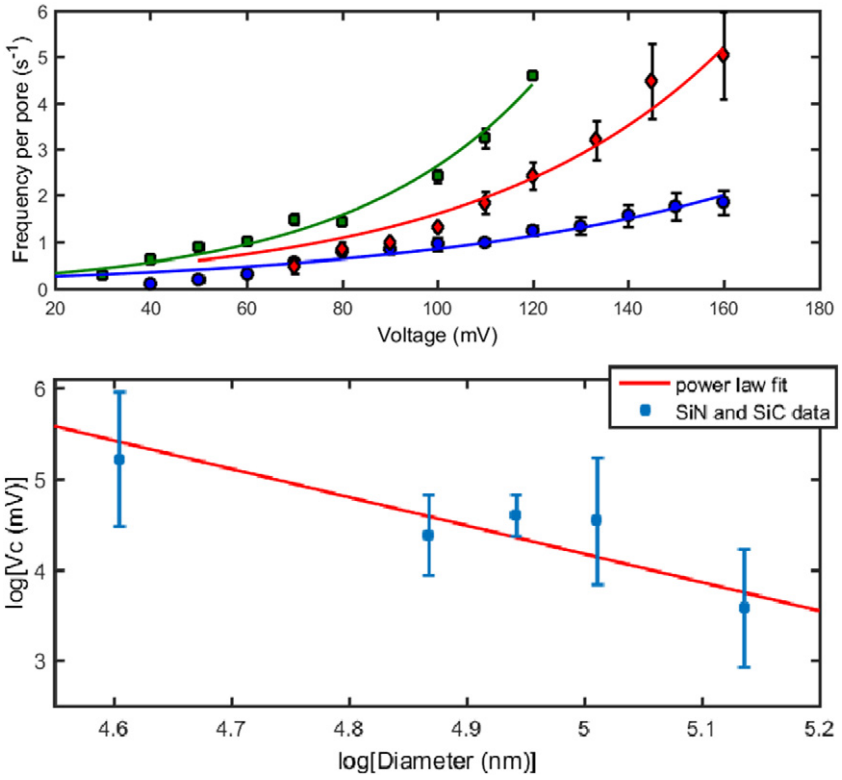

Fig. 4. Characterisation of transport of phage λ DNA molecules through the NZMW device. (A) Frequency-Voltage relationship for λ-DNA translocations through arrays of nanopores fabricated in gold-coated SiN. Blue: 100 nm diameter nanopores; Red: 130 nm; Green: 140 nm. Solid line fit by the electrical suction model. (B) Critical voltage as a function of the diameter of the pore on a loglog scale. Solid line: power law fit (exponent extracted: -3 ± 0.1).

has been determined in other studies [23–25] and in this case scales as:

$$f_e \frac{c\pi D^2 \mu}{4l} \Delta V \tag{3}$$

With c being the concentration of DNA molecule in the entrance compartment and μ being the electrophoretic mobility of DNA.

Finally, the frequency of translocation or capture rate per pore is given by:

$$f = f_e e^{-\Delta F/k_B T} = \frac{c\pi D^2 \mu}{4l} \Delta V \cdot e^{-V_c/\Delta V} \tag{4}$$

This description is valid for the electrical injection of polymers with a radius of gyration larger than the pore diameter and in the dilute regime.

From the fitting procedure with Eq. (4), the evolution of the critical voltage as a function of the diameter was extracted. It is in good agreement with a drift limited injection (critical voltage scales as D^α with $\alpha = -3 \pm 0.1$) and a constant surface charge for the injected blobs (access frequency scales as D^β with $\beta = 2 \pm 0.1$).

4. Conclusions

In this work we have demonstrated that simple NZMW devices can be fabricated in a gold-covered dielectric by FIB patterning. The procedure can be carried as a batch process and hundreds of devices can be fabricated within a single patterning run.

We have used NZMW devices containing arrays of nanopores of different sizes to investigate the translocation of fluorescently labelled DNA molecules and we have shown how the frequency of translocation events and the critical voltage vary with pore size. Our data is in good agreement with drift-limited injection of DNA into the nanopores and is also in agreement with DNA molecules behaving as blobs with a constant surface charge.

Finally, we note that our NZMW devices can be fabricated in a simple and reproducible batch process. We hope that these can become the platform for a new generation of nanopore devices.

Supplementary data to this article can be found online at https://doi.org/10.1016/j.mee.2017.12.005.

Acknowledgements

The authors acknowledge the enormous contributions made by Loïc Auvray (1956–2016) to: the fields of soft matter and biological physics; to European science as a whole; and to supporting the careers of younger researchers (the authors among them).

Funding

J.Y. was financially supported by the Fundação para a Ciência e a Tecnologia (FCT, Portugal) Postdoctoral Fellowship SFRH/BPD/80071/2011, through European Union and National funds and co-funded by Human Capital Operating Programme (*Programa Operacional do Capital Humano*, POCH).

This work was supported by the ANR project Golden Gates (ANR-14-CE08-0011).

References

[1] J.J. Kasianowicz, E. Brandin, D. Branton, et al., Characterization of individual polynucleotide molecules using a membrane channel, Proc. Natl. Acad. Sci. U. S. A. 93 (1996) 13770–13773.

[2] J.W.F. Robertson, C.G. Rodrigues, V.M. Stanford, et al., Single-molecule mass spectrometry in solution using a solitary nanopore, Proc. Natl. Acad. Sci. U. S. A. 104 (2007) 8207–8211.

[3] M. Pastoriza-Gallego, L. Rabah, G. Gibrat, et al., Dynamics of unfolded protein transport through an aerolysin pore, J. Am. Chem. Soc. 133 (2011) 2923–2931.

[4] C. Plesa, D. Verschueren, S. Pud, et al., Direct observation of DNA knots using a solid-state nanopore, Nat. Nanotechnol. 11 (2016) 1093–1097.
[5] M. Jain, H.E. Olsen, B. Paten, et al., The Oxford nanopore MinION: delivery of nanopore sequencing to the genomics community, Genome Biol. 17 (2016) 239.
[6] B. McNally, A. Singer, Z. Yu, et al., Optical recognition of converted DNA nucleotides for single-molecule DNA sequencing using nanopore arrays, Nano Lett. 10 (2010) 2237–2244.
[7] T. Gilboa, A. Meller, Optical sensing and analyte manipulation in solid-state nanopores, Analyst 140 (2015) 4733–4747.
[8] B.N. Anderson, O.N. Assad, T. Gilboa, et al., Probing solid-state nanopores with light for the detection of unlabeled analytes, ACS Nano 8 (11) (2014) 11836–11845.
[9] A. Ivankin, R.Y. Henley, J. Larkin, et al., Label-free optical detection of biomolecular translocation through nanopore arrays, ACS Nano 8 (2014) 10774–10781.
[10] V.V. Thacker, S. Ghosal, S. Hernández-Ainsa, et al., Studying DNA translocation in nanocapillaries using single molecule fluorescence, Appl. Phys. Lett. 101 (2012), 223704.
[11] V. Kurz, E.M. Nelson, J. Shim, et al., Direct visualization of single-molecule translocations through synthetic nanopores comparable in size to a molecule, ACS Nano 7 (2013) 4057–4069.
[12] G.V. Soni, A. Singer, Z. Yu, et al., Synchronous optical and electrical detection of biomolecules traversing through solid-state nanopores, Rev. Sci. Instrum. 81 (2010), 14301. .
[13] J.K. Rosenstein, M. Wanunu, C.A. Merchant, et al., Integrated Nanopore Sensing Platform With Sub-microsecond Temporal Resolution, 9, 2012.
[14] W.H. Pitchford, H.J. Kim, A.P. Ivanov, et al., Synchronized optical and electronic detection of biomolecules using a low noise nanopore platform, ACS Nano 9 (2015) 1740–1748.
[15] D.H. Russell, The waveguide below-cutoff attenuation standard, IEEE Trans. Microw. Theory Tech. 45 (1997) 2408–2413.
[16] M.J. Levene, J. Korlach, S.W. Turner, et al., Zero-mode waveguides for single-molecule analysis at high concentrations, Science 299 (2003) 682–686.
[17] K. Nakano, A. Shiroma, M. Shimoji, et al., Advantages of genome sequencing by long-read sequencer using SMRT technology in medical area, Hum. Cell 30 (2017) 149–161.
[18] J. Larkin, R.Y. Henley, V. Jadhav, et al., Length-independent DNA packing into nanopore zero-mode waveguides for low-input DNA sequencing, Nat. Nanotechnol. (2017) 1–8.
[19] J. Larkin, M. Foquet, S.W. Turner, et al., Reversible positioning of single molecules inside zero-mode waveguides, Nano Lett. 14 (2014) 6023–6029.
[20] T. Plénat, S. Yoshizawa, D. Fourmy, DNA-guided delivery of single molecules into zero-mode waveguides, ACS Appl. Mater. Interfaces 9 (2017) 30561–30566.
[21] T. Auger, J. Mathé, V. Viasnoff, et al., Zero-mode waveguide detection of flow-driven DNA translocation through nanopores, Phys. Rev. Lett. 113 (2014), 28302. .
[22] J. Gierak, Focused ion beam nano-patterning from traditional applications to single ion implantation perspectives, Nano 1 (2014) 35–52.
[23] S.E. Henrickson, M. Misakian, B. Robertson, et al., Driven DNA transport into an asymmetric nanometer-scale pore, Phys. Rev. Lett. 85 (2000) 3057–3060.
[24] M. Wanunu, W. Morrison, Y. Rabin, et al., Electrostatic focusing of unlabelled DNA into nanoscale pores using a salt gradient, Nat. Nanotechnol. 5 (2010) 160–165.
[25] A. Meller, D. Branton, Single molecule measurements of DNA transport through a nanopore, Electrophoresis 23 (2002) 2583–2591.